Toward battery-free flight: Duty cycled recharging of small drones

Nishant Elkunchwar[1], Suvesha Chandrasekaran[1], Vikram Iyer[2], and Sawyer B. Fuller[1]

***Abstract*— Constrained battery life on current Unmanned Aerial Vehicles (drones) limits the time they can operate and distance they can travel. We address this challenge by harvesting solar power to enable duty-cycled operation on a palm-sized drone. We present a scaling analysis that suggests that more solar power can be collected per unit mass of the drone as scale reduces, favoring small drones. By charging from the sun, the drone can operate for more than a single charging cycle, enabling extended mission time, and long-distance travel. To realize this, we design a high efficiency charging circuit and introduce two innovations. The first is a photovoltaic array that passively folds down while in flight to reduce air drag and automatically opens during landing due to the ground effect. The second is a sensor system and controller that autonomously finds suitable charging sites that are flat and well-lit. The drone can be fully charged in 3 hrs using the solar array and charging circuit with an average efficiency of 90.84%. Each charge enables a 4.7 min flight, allowing the drone to travel up to 1.2 km in a day. We also discuss how this platform could be used to take periodic measurements for smart agriculture or wildlife tracking, rapidly deploy wireless networks, or deploy microrobots in the future.**

I. Introduction

Unmanned Aerial Vehicles, also known as UAVs or drones, have begun to transform a variety of fields. They can enable rapid surveys of large areas for smart agriculture [1], [2], [3], wildlife conservation [4], and serve as a platform for carrying novel sensors [5], to name a few examples.

Current UAV platforms however have short operational lifetimes which limit their utility. This is due to the low energy density of available battery technologies and the high energy cost for flight. In this work we seek to address this challenge by using miniaturization to reduce the latter and using solar energy harvesting to recharge an on-board battery (Fig. 1), significantly increasing the drone's airtime [6].

To understand why solar power may be advantageous for small robots, consider the physics of scale as robot size diminishes. For a robot measuring ℓ from propeller tip to propeller tip, its "scale" is ℓ. A cube of length ℓ has surface area $6\ell^2$, volume ℓ^3, and mass $m = \rho\ell^3$ where ρ is its density. Neglecting constants to emphasize scale effects, we can say that area scales with ℓ^2 or area $\sim \ell^2$, and volume and mass $\sim \ell^3$. Solar power favors small scale because of its high surface-area-to-volume ratio: array area $\sim \ell^2$ while power needed varies with mass $\sim \ell^3$.[3] Therefore, the relative amount of power available from solar photovoltaics scales as ℓ^{-1}, favoring reduced scale. This trend can be observed in physical drones: If drone mass, size, and photovoltaic size required to power continuous hovering flight are plotted, they follow equivalent power laws (Fig. 2). To create this plot, we considered drones capable of sensor-autonomous hovering, assumed $\frac{1}{3}$ sun and 30% efficient cells.

Trend lines associated with these two scaling laws are given by $m = \alpha_2\ell^2$ and $m = \alpha_3\ell^3$. We fit free parameters α_1 and α_2 to mass m, characteristic length ℓ,

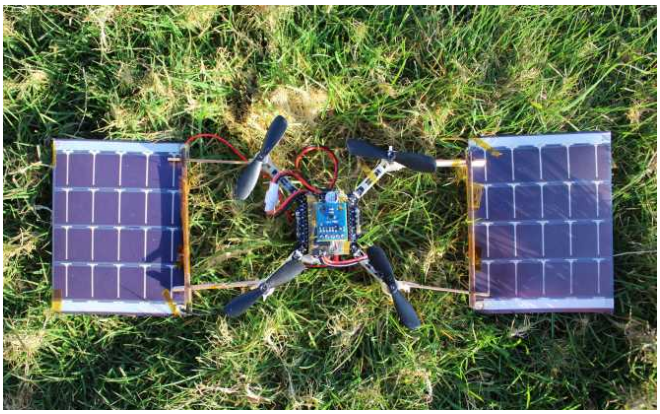

Fig. 1: The palm-sized drone carries two lightweight solar panels, a maximum-power-point tracking charging circuit, and a sensor package that allows it to fly autonomously and detect suitable sites for charging.

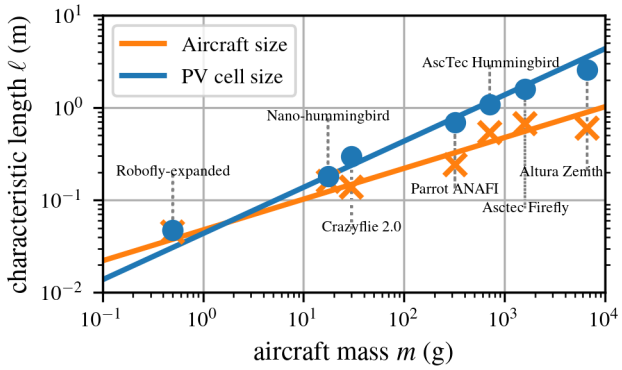

Fig. 2: Photovoltaic (PV) powered hovering favors small aircraft because of physical scaling effects. PV size needed for continuous hovering flight in $\frac{1}{3}$ sun falls below robot size below about 1 g.

[1]Department of Mechanical Engineering, University of Washington, Seattle, WA, USA

[2]Paul G. Allen School of Computer Science and Engineering, University of Washington, Seattle, WA, USA

[3]For small scale, power reduces slightly faster, making this conservative. Assuming inviscid flow, helicopter disc-loading theory [7] dictates that power $p = (mg)^{\frac{3}{2}}/\sqrt{2\rho A} \sim \ell^{3\frac{1}{2}}$, where g is the gravitational constant, ρ is air density, and $A \sim \ell^2$ is the area swept by the rotors.

Aircraft	Mass (g)	Power (W)	PV size (m)
Aerialtronics Zenith [9]	6650	666	2.58
AscTec Firefly [10], [11]	1600	251.03	1.58
AscTec Hummingbird [12]	710	116.55	1.08
Parrot ANAFI [13]	320	47.95	0.69
Crazyflie 2.0 [14]	30	8.88	0.30
Nano-hummingbird [15]	17.5	3.27	0.18
Robofly-expanded [16]	0.5	0.22	0.05

TABLE I: PV cell size needed for continuous solar-powered hovering for various UAVs. Power requirements were estimated using battery capacity and flight time except for robofly-expanded and nano-hummingbird where the power requirements were provided in the respective papers. The Robofly mass is estimated for a configuration consisting of a 143 mg mechanism [16], 100 mg boost converter [17], a 100 mg battery [18], and a 150 mg sensor package

and required photovoltaic array size ℓ_a (where ℓ_a is the length on one side of a square array) for all data points k according to $\alpha_2 = \text{argmin } \Sigma_k \left(\log(\alpha_2 \ell_{ak}^2) - \log m_k\right)^2$ and $\alpha_3 = \text{argmin } \Sigma_k \left(\log(\alpha_3 \ell_k^3) - \log m_k\right)^2$. The trend lines suggest that array size needed for continuous flight falls below vehicle size at around 1 g. For this analysis, we neglected photovoltaic mass because we anticipate that drones will be powered by ultra-thin photovoltaics that have been realized in the laboratory as thin as 1–10 μm [8].

We observe that while there still exists a gap between currently available drone platforms and the light-weight high-efficiency solar panels required for continuous flight, this is a similar challenge seen in battery-free internet of things (IoT) sensors. Radio communication often dominates the power budget of these devices, however many IoT radios support ultra low power sleep modes that allow for duty-cycled operation at very low average power. In this work we take inspiration from this approach to design a system that uses solar recharging to enable duty-cycled operation of a palm-sized drone. We present an end-to-end system design for duty-cycled recharging including a solar power harvester and battery charging circuit, a passive hinge mechanism to allow the panels to fold up upon take-off and re-extend for charging upon landing, and a computationally efficient method for safe landing site detection. This approach allows for extended flights, periodic operation, and enables robust operation in a variety of light conditions.

Designing this system requires addressing a number of challenges. While miniaturization reduces the power required to fly, small drones such as the CrazyFlie also have a limited payload of 15 g. To operate within these constraints, we designed a lightweight solar cell array and harvesting circuit with maximum power point tracking (MPPT) that weighs 1.83 g. The charging circuit has an 90.84% average charging efficiency across varying light levels. We performed tests in real-world outdoor lighting conditions with varying sunlight intensity due to intermittent clouds and show that the battery can be fully recharged in 3 hrs.

In addition to minimizing weight, we must also consider the physical attachment of the solar cell to make sure the drone can still take off and perform flight control. Attaching large, flat solar arrays can affect airflow of the propellers and the robot's stability. To enable takeoff and controlled, stable flight, we design a light-weight mounting structure that enables maximal airflow and a passive hinge mechanism that allows the solar array to fold inwards on takeoff and deploy again upon landing.

To demonstrate end-to-end operation, we also consider the landing sequence required for recharging. We develop a computationally efficient means of surveying a landing site for safety to enable automated landing to recharge upon reaching a low battery threshold.

II. Related work

While tethered powering [19], [20] of UAVs can help mitigate the low battery capacity problem for surveillance in a small area, the drone's movement is severely restricted by the tether. Wireless power transfer [21] using stationary [22] or mobile [23], [24] base stations, as well as networks of base stations [25], requires the drone to search for and align with charging pads, which necessitates bulky sensors and computational capabilities for autonomous drones or pre-computed fixed locations, in addition to planning for the mobile base stations [24]. Similar requirements arise for autonomously docking robots to electrical outlets for charging ground robots [26], [27] or hot-swapping UAV batteries [28]. Solar-assisted flight has been explored for larger drone platforms [29], [6] however their size (> 1.6 m) significantly increases their cost, and their size limits utility for many applications. Additionally these designs are fragile as they use large arrays of unpackaged monocrystalline solar cells, and are cannot perform agile maneuvers due to their large flat form factor.

While fixed-wing aircraft possess the appropriate flight power, size and weight to be continuously powered by existing solar panels [30], they cannot be used for applications that require hovering flight. A prototype for a fixed wing aircraft which can be reconfigured as a drone was developed in [31]; however, experimental validation of the system's transition between states was not demonstrated in-flight.

III. System design

Our end-to-end system to enable duty-cycled recharging of a drone consists of three main components: a solar array and charging circuit to harvest energy, an attachment mechanism and hinge to hold the solar cells, and a computationally efficient method for safe landing site detection that can run onboard the drone. We explain the design of each of these components in detail below.

A. Components

We design our platform around a 21 g palm-sized drone platform (Crazyflie 2.1 [32]). While this small drone lies slightly above the 1 g threshold for continuous solar powered flight (Section I), augmenting it with solar power harvesting can enable periodic flights for sensing tasks, longer flight distances by pausing to recharge, and operation in the absence of power infrastructure.

Component	Weight (g)
Drone	21.12
Two solar Panels [MPT4.8-75]	3.96
Mounting mechanism	0.83
Charging circuit	1.83
Battery	8.16
Optic flow deck	1.73
Multiranger deck	2.30
BH1750 light sensor	0.80
Total	40.73

TABLE II: Weights of the components used in this work

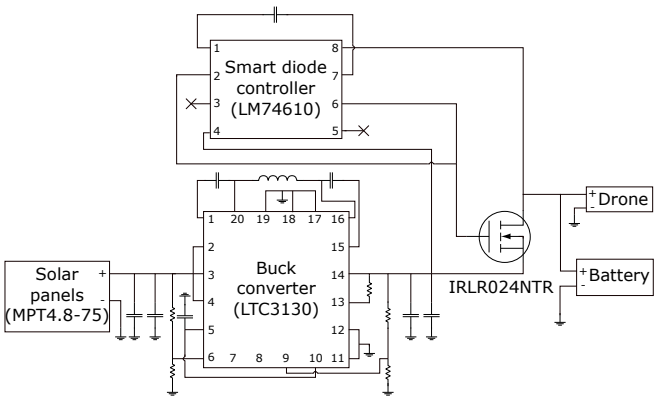

Fig. 3: Charging circuit schematic

To design this system we require a thin, lightweight photovoltaic array and charging circuit. To build this we use thin film, flexible. amorphous silicon cells (Powerfilm Inc.). The cells are 200 μm thick which makes them lightweight. Additionally, their flexibility makes them robust to damage. Each cell measures 94 mm $\times$ 73 mm and supplies power at up to 0.13 W/g in 1 sun. Each panel is rated for an operating current of 50 mA, an operating voltage of 4.8 V, and an open-circuit voltage of 7.4 V. Combining two of these cells would give a maximum power of 0.48 W and allow for recharging the drone in 3 hrs.

The output of solar cells however varies with amount of sunlight available, and non-ideal power sources like solar panels have characteristic voltage-current curves [33]. Extracting maximum power from a solar cell requires controlling its voltage by actively varying the load, in this case the battery charging rate. Additionally, the solar cells output 4.8 V while a fully charged LiPo battery has a maximum voltage of 4.2 V. To optimize battery charging, we design a harvesting circuit that achieves both voltage conversion and load variation for maximum power point tracking (MPPT).

We design this circuit using an Analog Devices LTC3130 buck converter which can tolerate input voltages up to 25 V which covers the full output range of the solar cell, and it can be configured to perform MPPT. The high voltage allows for a number of potential solar cell configurations of different sizes in series or parallel. Because our design uses two cells which will be placed flat on either side of the drone and will likely operate in similar light conditions, we connect them in parallel to allow the MPPT controller to regulate them to the same voltage.

While the buck converter chip produces an output capable of charging the battery, in low lighting conditions when the solar cell output falls too low, we need a solution to prevent battery discharge. To protect against this undervoltage condition, we added an N-channel MOSFET (IRLR024NTR, International Rectifier) with a smart diode controller (LM74610, Texas instruments) to function as an ideal diode. This overcomes the disadvantage of forward conduction voltage drop in case of Schottky diodes and also the addressees the inefficiency of PFETs at handling high load current at low input voltages. No overcurrent protection was required since the maximum possible current from our solar array is 200 mA, which is significantly lower than the maximum 2 C charging rate allowed for the 240 mA battery on the drone. Fig. 3 shows the schematic of the full charging circuit. The complete fabricated circuit measures 39 mm $\times$ 21 mm and weighs 1.83 g. Table II shows the all of the components used in this work and their corresponding weights.

B. Folding solar panel mounts

In addition to designing a charging circuit to harvest power, our solar array and charging circuit need to be mounted to the drone as well. This introduces a number of challenges. We observed that if the cells are placed above or too close to the propellers, they significantly reduce airflow and therefore lift. One solution is to create a frame that holds the panels further away from the propellers. We observed however that mounting a mass this far from the center of the robot causes instability during takeoff. Although the mass is within the payload specs of the drone, in a series of 12 tests it was only able to successfully lift off 25% of the time (see results). Additionally, we observed that the drone was unstable and quickly crashes.

To address this we designed a passive hinge mechanism that allowed the solar panels to fold downward as soon as the drone lifts off. Folding in this way reduces the horizontal surface area and hence the total drag. In addition to folding inward, the panels passively fold back out when the robot lands. We designed the mechanism so the robot could take off at 70% thrust. This was calculated after accounting for the weight of the circuitry, solar array, and the recommended payload capacity of 15 g of the drone.

We mounted two solar panels to the sides of the drone, using lightweight beams to hold them 4.5 cm away from the drone to avoid blocking the the downwash of the propellers. The beams were constructed from 2.3 mm balsa and machined using a CO_2 laser. They were bonded to the drone's motor sleeves using hot-melt glue (ethyl vinyl acetate). We created a flexure joint between the balsa structure and the PV array using adhesive-backed polyimide film (Kapton). This hinge was placed as high as possible to minimize the vertical distance between the center of pressure of the folded PV panels and the drone's center of mass. This minimizes the torque that occurs due to drag as the drone moves laterally.

The complete panel mounting solution is shown in Figure 4. The beams were interlocked using a press fit into a

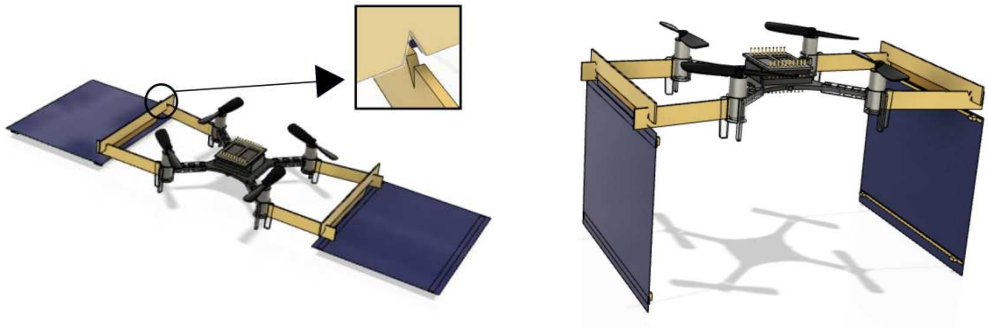

(a) (b)

Fig. 4: Solar panel support structure and mechanism by which they fold downward during flight, mounted on the Crazyflie model [34]. (a) On the ground, the panels lay flat to collect the sun. Inset shows press-fit mechanism used to interlock balsa support structure. (b) Upon takeoff, flexure-based hinges allow the panels to fold downward, facilitating stable flight by reducing the drone's moment of inertia.

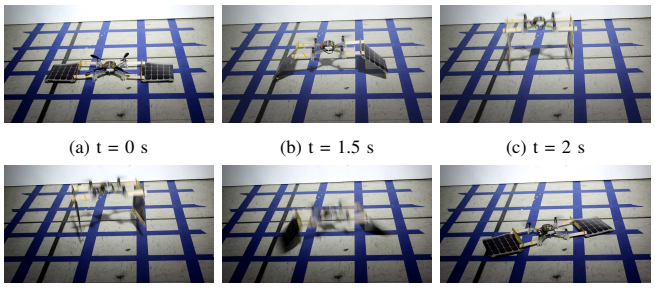

(a) t = 0 s (b) t = 1.5 s (c) t = 2 s

(d) t = 2 s (e) t = 2.4 s (f) t = 2.6 s

Fig. 5: A sequence of frames taken from a video of a single flight in which the drone took off and then subsequently landed after performing a short automated maneuver in the air. (a–c) During takeoff, the photovoltaic panels fold down passively. (d–f) During landing, the panels fold out automatically as well due to aerodynamic pressure under the drone due to the ground effect. Note that the landing sequence occurs over a much shorter period of time.

small V-notch inspired by techniques in wood-working that leverage the pliability of the wood to create press-fit joints without the need for fasteners. We then reinforced the joints with a thin layer of cyanoacrylate glue. We added small feet-like projections to the base of the distal ends of the panels to ensure they were level when the drone is on the ground.

To open the panels when the drone lands, we take advantage of the ground effect, which is an increase in air pressure that occurs below the drone when it is near the ground. This causes the panels to push outward as the drone descends, so that they lie flat upon landing.

C. Safe Landing Procedure

The section above describes a mechanical design that enables safe liftoff and flight with the solar array, however because the solar cells are folded inward and the flight time is shorter than the charging time, our system also requires a safe landing strategy. Before landing the drone must be able to detect obstacles at the landing site.

A flat terrain check for drone landing has previously been demonstrated using a camera and LIDAR [35], [36], however these systems required components that are far too heavy for a palm-sized drone. Moreover, these methods are computationally intensive.

Our solution instead consists of a simple strategy of collecting distance measurements using a downward facing VL53L1X time-of-flight rangefinding sensor already present on the drone. The drone performs a small maneuver over the ground and decides whether the terrain is safe by analyzing the standard deviation of those measurements. [37] uses a similar method but requires human operators to select the threshold. We chose a fixed threshold of 15 mm based on experiments performed on various surfaces.

Additionally to maximize the charging rate we would like to land the drone in a location with a minimum threshold light intensity, so that it avoids shaded areas. The threshold was chosen to be 1000 lux for indoor experiments and 100,000 lux (1 sun) for outdoor experiments. To do this, we use a light intensity sensor (BH1750, ROHM Semiconductor) along with a driver developed in [38]. We choose a final landing site that has a light intensity above the desired threshold as well as one that is determined to be flat as per the standard deviation of the downward-facing time of flight sensor measurements.

IV. Results

The video accompanying the paper shows the flight performance and landing site selection algorithm. We evaluate each component of our system below.

Solar charging. To evaluate the solar cells and charging circuit described in section III to charge the drone's LiPo battery, we placed the solar array and charging circuit flat on the ground outdoors under sunlight with light intensity varying with the time of day and presence of clouds to measure performance in real world light conditions. We measured the current and voltage at the input and output of the charging circuit using digital multimeters (Fluke 287) and measured light intensity using a digital lux meter (Fluke 941) placed next to the panels, every 5 min. While data was collected manually for these experiments future versions could integrate voltage, current and light sensing with the drone telemetry. Fig. 6 shows the battery voltage, charging

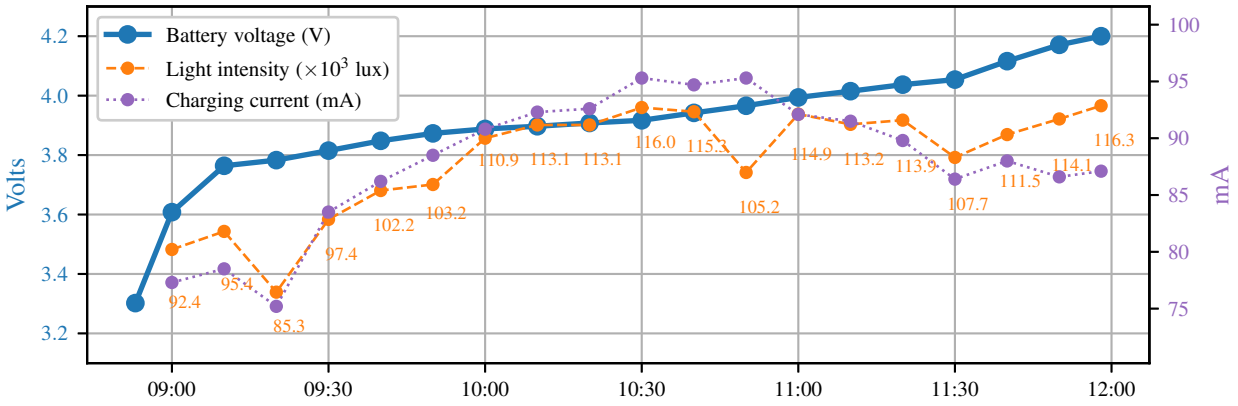

Fig. 6: Battery voltage and charging current variation with light intensity for a complete charge cycle. The first datapoint is open-circuit voltage, rest are while battery is connected and charging

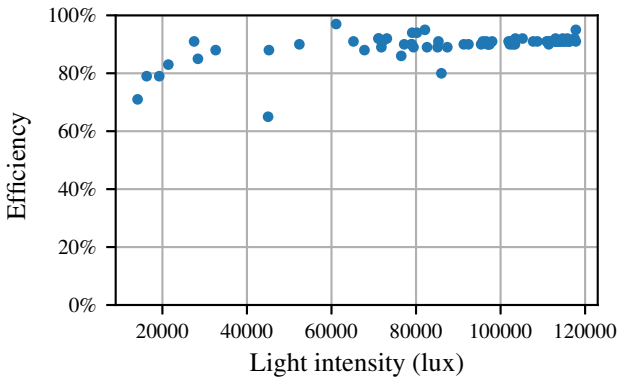

Fig. 7: Efficiency of the charging circuit varies with received sunlight intensity. The circuit is more efficient for higher amount of light

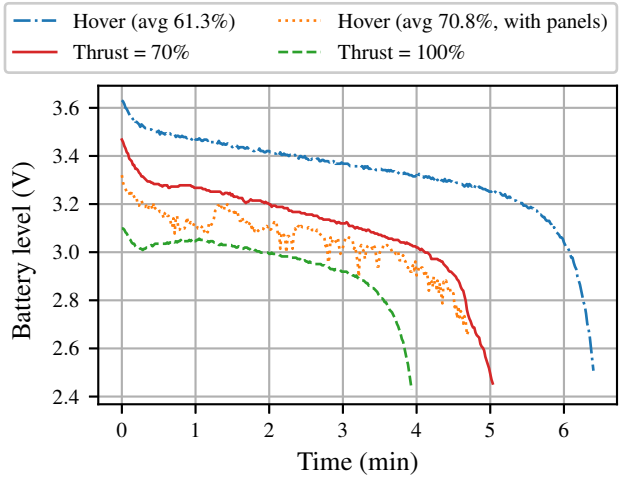

Fig. 8: Plot of battery voltage with thrust levels

current output to the battery and sunlight intensity variation for one complete charge. The total charging time for this test was 3 hrs 3 min. Using the input and output power measurements, we calculate the charging circuit's efficiency shown in Fig. 7. While the efficiency varies with light intensity, it is consistently above 60%, with an average 90.84% for the experiment. We note that solar cell output scales non-linearly with light intensity, and expect the charging time to be even lower for bright, sunny days due to more light as well as increased charging efficiency at higher light levels (fig. 7.) The maximum recorded light intensity over the experiment was 117800 lux and the average intensity was 107162 lux (just over 1 sun).

We also evaluated different solar array sizes to provide empirical measurements of the scaling trends described in Fig. 2 and demonstrate potential solutions for drones with higher payload capacity. We performed these experiments in real outdoor lighting conditions, tabulating the average light intensity along with these results in Table III. The results show the charging time could be decreased to less than 1.5 hrs. This suggests a higher duty cycle is possible on clear days. The scaling when doubling the array size by using four MPT4.8-75 cells is approximately linear as expected. We note, however, that charging with the larger MPT6-75 cells was measured under lower light due to weather constraints resulting in only a small decrease in charging time.

Flight performance. We next evaluated the drone's ability to take off while carrying the PV cells. As shown in Fig. 5, the drone is able to lift off and the cells fold downward. We performed 12 flights on a drone equipped with the hinge-based panel folding mechanism. We observed consistent, stable flight and autonomous maneuvers in all trials at speeds of up to 1.4 m/s. To determine if folding is needed, we performed 12 additional flights on a drone in which the cells held rigidly outward. The drone was only able to successfully take off in 3 out of 12 trials (25% success rate). This is due to disruption of airflow and higher drag when panels are oriented laterally under the rotors as well as the large torques caused by mounting panels away from the center of

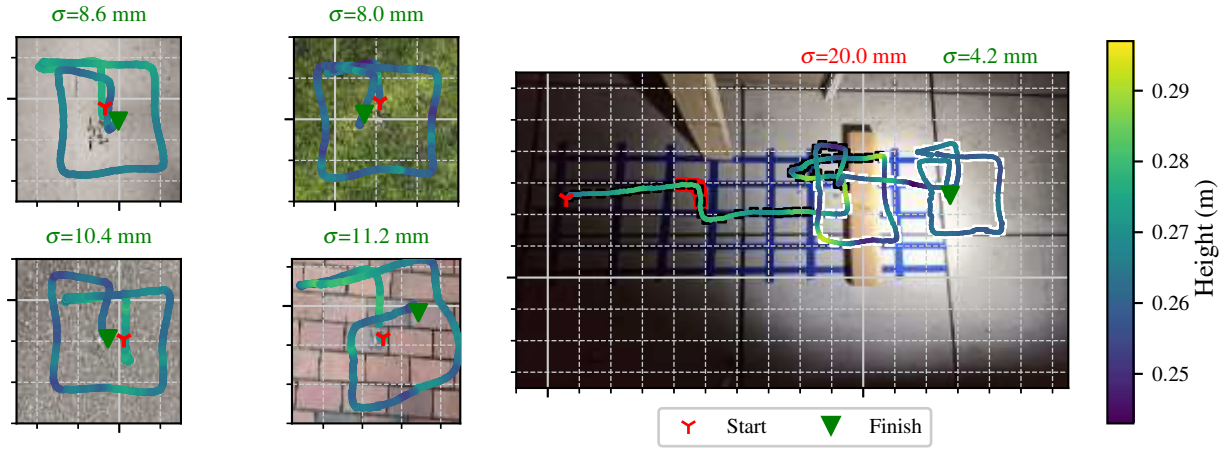

Fig. 9: (left) Measured flatness over various surfaces. Moving clockwise from the top the surfaces are: terrazzo tiles, short grass, concrete paver tiles, gravel. (right) Automated landing site suitability detection. The drone searches for a site with enough light (a black background under the trajectory indicates insufficient light, < 1000 lux) that is flat. It also avoids nearby obstacles by detecting them with laterally-oriented laser rangefinders (red background under the trajectory). Once the light intensity is greater than the chosen threshold (white background), the drone moves in a square trajectory around the area to be tested for flatness. If the standard deviation of the time of flight measurements over the square is greater than a heuristic threshold, it keeps searching for another landing area. Finally, the drone lands when it has found a suitable site.

Panels	Mass (g)	Average light intensity ($\times 10^3$ lux)	Average charging efficiency	Charging time (min)
two MPT4.8-75	3.96	107.16	90.84%	183
four MPT4.8-75	7.92	71.41	89.61%	84
four MPT6-75	9.20	65.74	86.94%	80

TABLE III: Time taken to recharge a battery from 3.3 V to 4.2 V for different cell configurations and lighting conditions

mass which disrupt the controller and cause instability.

To estimate total flight time of the drone, we recorded the battery voltage starting from full charge for two fixed thrust levels as well as the thrust required to hover with and without the solar array. Data was recorded using the python library provided by the drone manufacturer [39] which also contains logging functionality. Fig. 8 shows the resulting discharge curves. At the hover thrust required when lifting, the drone can fly for about 4.7 min. When flying at maximum velocity this enables flight distances of approximately 400 m.

Landing site selection. We demonstrated that it is possible for the drone to use its on-board sensor suite, plus a light sensor, to detect suitable landing sites. Fig. 9 shows an example of our algorithm in operation. Our system detects whether there is light present and whether the terrain is flat enough to ensure that the drone can take off again and the panels will lie flat. Fig. 9 shows example flatness test trajectories on different terrain such as grass and rocks, including an example trial in which the drone automatically rejected two sites because they were too dark or had uneven terrain (wooden block placed as an obstacle) . To initiate the autonomous landing sequence, a conservative threshold of 2.8 V was used based on the discharge curve at 100% thrust (fig. 8). The drone records battery voltage on-board. Since any non-zero thrust induces a voltage sag, choosing a threshold based on the 100% thrust curve ensures that transient voltage sags due to thrust changes during hovering do not cause an accidental early landing decision. Another strategy to minimize transients can be to calculate a moving average of the last few voltage measurements.

The flat site selection process described in this work was designed considering the limited payload, power and computational capabilities of the platform and hence has some limitations. Firstly, since flatness is measured with a downward facing time-of-flight sensor, any factors that might cause changes in the drone's height (for example payload near maximum payload limit, low battery, etc) will be registered as unflat terrain. Secondly, while executing a reference trajectory like a square used in this work, the localization estimate is obtained from the drone's estimator based on measurements from an inertial measurement unit, an optic flow sensor and a downward-facing range finder. This position estimate performs poorly on plain, featureless surfaces, or surfaces with repetition as can be seen in the case of concrete paver tiles in fig. 9. For better location estimation, ultra-wide bandwidth based location estimation [40], SteamVR based localization [41] and MotionCapture localization [42] are supported by the drone manufacturer with the platform firmware [43].

V. Conclusion

This paper presents a drone recharging system using thin, lightweight solar panels, enabling duty-cycled operation without any human intervention. This approach avoids the need for a complex autonomous battery replacement system and associated planning and docking. We demonstrate an end-to-end design including a 1.83 g, 90.84% efficient power

harvesting circuit, passive folding mechanism to enable stable flight with the solar array, and landing site selection algorithm. The solar panels and mounting mechanism constitute about 11.7% of the total mass of the platform. We show this system can fully charge the drone within 3 hrs 3 min in real world light conditions to enable a 4.7 min flight.

Our results support two main conclusions. The first is that solar power favors small size. And the second is that it is possible, though appropriate design of a deployable photovoltaic array, charging circuit, and landing site selection, for small robots to operate for much longer than is possible on a single battery charge. This serves as an important milestone toward battery-free, indefinite-time flight for aerial robots.

A number of advancements will facilitate drones with indefinite flight time. The first is to integrate more advanced photovoltaic cells. For example, 2.5% duty cycle demonstrated in this work could be dramatically increased by using technologies such as triple-junction Gallium Arsenide cells (e.g. MicroLink devices) which can exceed 30% efficiency and are only 40 μ m thick. Such cells provide a power density exceeding 1 W/g, which is greater than 7$\times$ that of the cells used in this work. This and future advances in photovoltaics allow us to move along and adjust the PV cell size line shown in Fig. 2. Second, there is room to improve the efficiency of the vehicle such as by using brushless motors and a lighter airframe. Lastly, our results suggest that a move to still smaller drones such as the insect-sized 150 mg UW Robofly [16] will allow operation at the left side of the intersection of the two lines in Fig. 2. In that regime, it may be possible to fly indefinitely with a PV array that is smaller than the physical dimension of the robot.

The system we demonstrated here could be used for a variety of applications in its current state. Specifically, solar power harvesting can enable long distance flights and remote operation with zero power infrastructure. We highlight three potential applications below.

Smart agriculture and aerial surveys. Emerging smart agriculture technologies such as Microsoft FarmBeats [1] requires capturing aerial images of a farm. This system would allow a single, low-cost drone to periodically fly and survey a field without any infrastructure, enabling use in a variety of environments including in developing countries with unreliable power. Additionally, the drone could either log data to an SD card [44], or transmit it using low-power wide-area network (LPWAN) technologies. These radios can transmit up to 17 km, weigh 613 mg, and can consume tens of milliwatts on average, which is significantly lower than flight [45]. This system would allow a drone to travel 6 times the distance with two 3-hour recharges (typical in one day). Flying at its default maximum velocity of 1.4 m/s the drone could travel about 1.2 km per day, which would allow it to traverse large farms or perform persistent aerial surveys needed for wildlife tracking [4]. Between flights the system can also double as a traditional IoT sensor node. Many environmental sensors are lightweight ($<$ 1.5 g), and low power ($<$ 1 mA) allowing them to run with minimal impact on charging: a temperature / humidity / pressure / VOC sensor (Bosch BME680 [46], $\approx$17 mg, 3.7 µA), light sensors (On Semi LV0104CS [47], 1.4 mg, 70 µA, [48]), a CO_2 gas sensor (Sensirion SCD40 [49], 0.55 g, 0.5 mA), electrochemical gas sensors (SPEC Sensors 100-102 [50], 1.4 g, 10-50 µW), a camera [51] (24 mg, $<$2 mW), a pressure sensor (Bosch BMP388 [52], 6.3 mg, 3.4µA).

Wireless network deployment. This system could also be used for rapid deployment of a wireless network in an emergency scenario. For example, if drones were equipped with a LoRa chipset that can weigh as little as 613 mg [45], they could be programmed fly to different locations. Upon landing, the solar power could be used to power the radios.

Microrobot deployment. This platform could also be used to enable deployment of microrobots in the future. For example, the drone could fly to a remote location and deploy one or a number of terrestrial or aerial microrobots to explore the environment. The large drone could act as a power source to recharge the small robots using its comparatively large area solar panels and serve as a communication base station to relay messages.

ACKNOWLEDGMENT

The authors would like to thank Yogesh Chukewad for insightful suggestions during the writing of this manuscript, and the Air Force Office of Scientific Research (AFOSR), grant no. FA9550-14-1-0398 by The Air Force Center of Excellence on Nature-Inspired Flight Technologies and Ideas (NIFTI) for providing the drone hardware used in this research.

REFERENCES

[1] D. Vasisht, Z. Kapetanovic, J. Won, X. Jin, R. Chandra, S. Sinha, A. Kapoor, M. Sudarshan, and S. Stratman, "Farmbeats: An iot platform for data-driven agriculture," in *14th {USENIX} Symposium on Networked Systems Design and Implementation ({NSDI} 17)*, pp. 515–529, 2017.

[2] U. R. Mogili and B. Deepak, "Review on application of drone systems in precision agriculture," *Procedia computer science*, vol. 133, pp. 502–509, 2018.

[3] Y.-H. Tu, S. Phinn, K. Johansen, A. Robson, and D. Wu, "Optimising drone flight planning for measuring horticultural tree crop structure," *ISPRS Journal of Photogrammetry and Remote Sensing*, vol. 160, pp. 83–96, 2020.

[4] K. Shah, G. Ballard, A. Schmidt, and M. Schwager, "Multidrone aerial surveys of penguin colonies in antarctica," *Science Robotics*, vol. 5, no. 47, 2020.

[5] A. Fitzpatrick, A. Singhvi, and A. Arbabian, "An airborne sonar system for underwater remote sensing and imaging," *IEEE Access*, vol. 8, pp. 189945–189959, 2020.

[6] C.-F. Lin, T.-J. Lin, W.-S. Liao, H. Lan, J.-Y. Lin, C.-H. Chiu, and A. Danner, "Solar power can substantially prolong maximum achievable airtime of quadcopter drones," *Advanced Science*, vol. 7, no. 20, p. 2001497, 2020.

[7] W. Johnson, *Helicopter theory*. Courier Dover Publications, 2012.

[8] M. S. Branham, W.-C. Hsu, S. Yerci, J. Loomis, S. V. Boriskina, B. R. Hoard, S. E. Han, and G. Chen, "15.7% efficient 10-μm-thick crystalline silicon solar cells using periodic nanostructures," *Advanced materials*, vol. 27, no. 13, pp. 2182–2188, 2015.

[9] A. C. U. A. Systems, "*Aerialtronics Altura Zenith Specsheet*," 16 Jun 2017.

[10] A. Technologies, "Ascending technologies firefly," 2015.

[11] A. Technologies, "Payload options & accessories," 2015.

[12] A. Technologies, "Ascending technologies hummingbird," 2015.

[13] P. D. SAS, "Parrot anafi specsheet," 4 Jun 2018.

[14] J. Förster, "System identification of the crazyflie 2.0 nano quadrocopter," B.S. thesis, ETH Zurich, 2015.

[15] M. Keennon, K. Klingebiel, H. Won, and A. Andriukov, "Development of the nano hummingbird: A tailless flapping wing micro air vehicle," in *AIAA Aerospace Sciences Meeting*, (Reston, VA), pp. 1–24, AIAA, 9–12 January 2012.

[16] D. Dhingra, Y. M. Chukewad, and S. B. Fuller, "A device for rapid, automated trimming of insect-sized flying robots," *IEEE Robotics and Automation Letters*, vol. 5, no. 2, pp. 1373–1380, 2020.

[17] J. James, V. Iyer, Y. Chukewad, S. Gollakota, and S. B. Fuller, "Liftoff of a 190 mg laser-powered aerial vehicle: The lightest wireless robot to fly," in *2018 IEEE International Conference on Robotics and Automation (ICRA)*, pp. 1–8, IEEE, 2018.

[18] M. Duduta, S. de Rivaz, D. R. Clarke, and R. J. Wood, "Ultra-lightweight, high power density lithium-ion batteries," *Batteries & Supercaps*, vol. 1, no. 4, pp. 131–134, 2018.

[19] S. Jung, Y. Jo, and Y.-J. Kim, "Aerial surveillance with low-altitude long-endurance tethered multirotor uavs using photovoltaic power management system," *Energies*, vol. 12, no. 7, p. 1323, 2019.

[20] S. Jung, Y. Jo, and Y.-J. Kim, "Flight time estimation for continuous surveillance missions using a multirotor uav," *Energies*, vol. 12, no. 5, p. 867, 2019.

[21] M. Lu, M. Bagheri, A. P. James, and T. Phung, "Wireless charging techniques for uavs: A review, reconceptualization, and extension," *IEEE Access*, vol. 6, pp. 29865–29884, 2018.

[22] T. Campi, S. Cruciani, M. Feliziani, and F. Maradei, "High efficiency and lightweight wireless charging system for drone batteries," in *2017 AEIT International Annual Conference*, pp. 1–6, IEEE, 2017.

[23] M. R. Hayajneh and A. R. E. Badawi, "Automatic uav wireless charging over solar vehicle to enable frequent flight missions," in *Proceedings of the 2019 3rd international conference on automation, control and robots*, pp. 44–49, 2019.

[24] E. Ali, M. Fanni, and A. M. Mohamed, "Design and task management of a mobile solar station for charging flying drones," in *E3S Web of Conferences*, vol. 167, p. 05004, EDP Sciences, 2020.

[25] A. Alsharoa, H. Ghazzai, A. Kadri, and A. E. Kamal, "Spatial and temporal management of cellular hetnets with multiple solar powered drones," *IEEE Transactions on Mobile Computing*, vol. 19, no. 4, pp. 954–968, 2019.

[26] M. C. Silverman, D. Nies, B. Jung, and G. S. Sukhatme, "Staying alive: A docking station for autonomous robot recharging," in *Proceedings 2002 IEEE International Conference on Robotics and Automation (Cat. No. 02CH37292)*, vol. 1, pp. 1050–1055, IEEE, 2002.

[27] S. Oh, A. Zelinsky, K. Taylor, *et al.*, "Autonomous battery recharging for indoor mobile robots," in *Proceedings of the australian conference on robotics and automation*, Citeseer, 2000.

[28] B. Michini, T. Toksoz, J. Redding, M. Michini, J. How, M. Vavrina, and J. Vian, "Automated battery swap and recharge to enable persistent uav missions," in *Infotech at Aerospace 2011*, p. 1405, 2011.

[29] C. S. Goh, J. R. Kuan, J. H. Yeo, B. S. Teo, and A. Danner, "A fully solar-powered quadcopter able to achieve controlled flight out of the ground effect," *Progress in Photovoltaics: Research and Applications*, vol. 27, no. 10, pp. 869–878, 2019.

[30] H. Ross, "Fly around the world with a solar powered airplane," in *The 26th Congress of ICAS and 8th AIAA ATIO*, p. 8954, 2008.

[31] R. D'Sa, D. Jenson, and N. Papanikolopoulos, "Suav: Q-a hybrid approach to solar-powered flight," in *2016 IEEE International Conference on Robotics and Automation (ICRA)*, pp. 3288–3294, IEEE, 2016.

[32] W. Giernacki, M. Skwierczyński, W. Witwicki, P. Wroński, and P. Kozierski, "Crazyflie 2.0 quadrotor as a platform for research and education in robotics and control engineering," in *2017 22nd International Conference on Methods and Models in Automation and Robotics (MMAR)*, pp. 37–42, IEEE, 2017.

[33] K. L. Kennerud, "Analysis of performance degradation in cds solar cells," *IEEE Transactions on aerospace and electronic systems*, no. 6, pp. 912–917, 1969.

[34] R. Shu, "Cad rendering of crazyflie." `https://github.com/rshum19/Crazyflie-CAD`, 24 April 2017.

[35] L. Chen, X. Yuan, Y. Xiao, Y. Zhang, and J. Zhu, "Robust autonomous landing of uav in non-cooperative environments based on dynamic time camera-lidar fusion," *arXiv preprint arXiv:2011.13761*, 2020.

[36] M. Mittal, A. Valada, and W. Burgard, "Vision-based autonomous landing in catastrophe-struck environments," *arXiv preprint arXiv:1809.05700*, 2018.

[37] A. Cesetti, E. Frontoni, A. Mancini, P. Zingaretti, and S. Longhi, "A vision-based guidance system for uav navigation and safe landing using natural landmarks," *Journal of intelligent and robotic systems*, vol. 57, no. 1, pp. 233–257, 2010.

[38] N. Elkunchwar, V. Iyer, M. Anderson, K. Balasubramanian, J. Noe, Y. Talwekar, and S. Fuller, "Bio-inspired source seeking and obstacle avoidance on a palm-sized drone," 2021. (in prep).

[39] Bitcraze, "crazyflie-lib-python github repository." `https://github.com/bitcraze/crazyflie-lib-python`, 4 Mar 2021.

[40] Bitcraze, "Loco positioning system." `https://www.bitcraze.io/documentation/system/positioning/loco-positioning-system/`, 2021.

[41] Bitcraze, "Lighthouse positioning system." `https://www.bitcraze.io/documentation/system/positioning/ligthouse-positioning-system/`, 2021.

[42] Bitcraze, "Motion capture positioning." `https://www.bitcraze.io/documentation/system/positioning/mocap-positioning/`, 2021.

[43] "GitHub repository for crazyflie-firmware." Available: `https://github.com/bitcraze/crazyflie-firmware/`. 2020.

[44] Bitcraze, "Micro sd card deck — bitcraze." `https://www.bitcraze.io/products/micro-sd-card-deck/`, 2021.

[45] InsightSIP, "Isp4520 smart lora and bluetooth low energy module with mcu and antennas." `https://www.insightsip.com/fichiers_insightsip/pdf/ble/ISP4520/isp_lora_DS4520_R6.pdf`, 2020.

[46] B. Sensortech, "Gas sensor bme680." `https://www.bosch-sensortec.com/products/environmental-sensors/gas-sensors/bme680/`, 2021.

[47] O. Semiconductor, "Lv0104cs ambient light sensor datasheet." `https://www.onsemi.com/pdf/datasheet/lv0104cs-d.pdf`, 2021.

[48] S. B. Fuller, M. Karpelson, A. Censi, K. Y. Ma, and R. J. Wood, "Controlling free flight of a robotic fly using an onboard vision sensor inspired by insect ocelli," *Journal of The Royal Society Interface*, vol. 11, no. 97, p. 20140281, 2014.

[49] Sensirion, "Co2 sensor scd4x." `https://www.sensirion.com/scd40/`, 2021.

[50] S. Sensors, "15x15 co sensor 1000 ppm for sensor 100-102." `https://www.spec-sensors.com/wp-content/uploads/2016/04/3SP_CO_1000-C-Package-110-109.pdf`, 2021.

[51] V. Iyer, A. Najafi, J. James, S. Fuller, and S. Gollakota, "Wireless steerable vision for live insects and insect-scale robots," *Science robotics*, vol. 5, no. 44, 2020.

[52] Bosch, "Bmp 388 digital pressure sensor datasheet." `https://www.bosch-sensortec.com/media/boschsensortec/downloads/datasheets/bst-bmp388-ds001.pdf`, 2021.